Journal of the Optical Society of America B
OPTICAL PHYSICS

Large electromagnetic field enhancement achieved through coupling localized surface plasmons to hybrid Tamm plasmons

HAI LIU,* JINSONG GAO, ZHEN LIU, XIAOYI WANG, HAIGUI YANG, AND HONG CHEN

Key Laboratory of Optical System Advanced Manufacturing Technology, Changchun Institute of Optics, Fine Mechanics and Physics, Chinese Academy of Sciences, Changchun 130033, China
**Corresponding author: nmliuhai@163.com*

Received 25 June 2015; revised 11 August 2015; accepted 11 August 2015; posted 17 August 2015 (Doc. ID 243322); published 4 September 2015

We theoretically demonstrate the coupling between localized surface plasmons (LSPs) and two types of hybrid Tamm plasmons (TPs) in a system consisting of a metallic nanowire array incorporated into a microcavity with an intracavity metal layer. Theoretical studies show that the interaction of the LSPs with these two hybrid TPs can be manipulated by changing the length of the cavity, and strong coupling between the LSPs and one of the hybrid TPs is observed, manifested by a huge anticrossing in the dispersion diagram. The coupling results in a surprisingly large splitting of 299 meV, as well as two branches of new hybrid TP-LSP modes. The hybrid TP-LSP modes feature both TP and LSP characteristics. The electric fields between the wire edges and the metal layer are significantly enhanced, and the magnetic fields are highly confined underneath the metal nanowires and to the interface of the metal layer. Furthermore, because of the coupling with the LSP, the coupling between these two hybrid TPs is also enhanced greatly in the considered structure. These findings hold promise in applications such as plasmon enhanced nonlinear nano-optics and reduction of lasing threshold in organic microcavities.

OCIS codes: (240.6680) Surface plasmons; (050.2230) Fabry-Perot; (250.5403) Plasmonics.

http://dx.doi.org/10.1364/JOSAB.32.002061

1. INTRODUCTION

Tamm plasmons (TPs) are a novel kind of surface electromagnetic waves supported at the interface of a metal layer and a distributed Bragg reflector (DBR) [1]. Contrary to surface plasmon polaritons (SPPs), TPs can be formed in both TE and TM polarizations, and possess an in-plane parabolic dispersion within the light cone. Therefore, they can be excited at all angles of incidence directly. Furthermore, the typical linewidth of TPs is one order of magnitude lower than the one of ordinary surface plasmons, resulting in higher surface fields and longer propagation distances, which makes them attractive for enhancing light-matter interaction at nanoscale. These remarkable properties of TPs open fascinating applications in resonant optical filters [2], bistable switching [3], and sensors [4].

In addition, the interaction of TPs with other resonances, such as excitons or microcavity modes, has also been explored in the last few years because of prospective applications in new compact lasers [5,6] and polariton integrated circuits [7]. In the case of incorporating a thin metal layer into a planar organic microcavity, a transition from a single cavity mode into two hybrid TP modes is observed [8,9]. The eigenenergies of these hybrid TP modes depend on both the thickness of the metal layer and the adjacent dielectric layers. By further structuring the metal layer incorporated into the cavity, macroscopic coherence [10] and strong lateral confinement [11] of light are observed, which can help in the realization of an electrically driven organic laser diode. The coupling between TPs and SPPs, as well as localized surface plasmons (LSPs), has also been theoretically explored in a multilayer structure consisting of a metallic nanowire array arranged on top of a metal layer-DBR structure [12]. Despite strong light confinements, the formed TP-SPP and TP-LSP hybrid states also exhibit extremely narrow linewidths and enhanced local fields. Experimental verification of the TP-SPP hybrid state was then reported in the Kretschmann configuration [13]. The advantage of the formed TP-SPP hybrid state is that it allows us to realize a highly sensitive and accurate sensor [14], and to efficiently out-couple and beam TPs [15]. However, in all these cases, TPs and SPPs (or LSPs) are excited at the two different interfaces of the metal layer. Coupling between TPs and SPPs (or LSPs) mainly relies on the frustrated decay of optical fields through the metal layer, which greatly limits the maximum coupling strength that can be achieved.

In this paper, we present a configuration in which a metallic nanowire array is incorporated into a microcavity with an intracavity metal layer. In addition to the LSPs being excited on metallic nanowires, two kinds of hybrid TPs can also be separately formed on the two interfaces of the intracavity metal layer, labeled as TP I and TP II, respectively [8]. Theoretical studies show that the interaction of the LSPs with these two kinds of hybrid TPs can be manipulated by changing the length of the cavity, and strong coupling between the LSPs and one of the hybrid TPs (TP I) is observed, manifested by a huge anticrossing in the dispersion diagram. The coupling results in a surprisingly large splitting of 299 meV, as well as two branches of new hybrid LSP-TP modes. Upon the excitation of the hybrid LSP-TP mode, the electric fields between the wire edges and the metal layer are significantly enhanced. Furthermore, the coupling between the two hybrid TPs is also enhanced greatly in the considered structure, which can be attributed to the strong confinement of the local fields near the intracavity metal layer produced by the incorporated nanowires.

2. SYSTEM DESCRIPTION

Our system consists of a metallic nanowire array incorporated into a microcavity with an intracavity metal layer, as shown in Fig. 1. The bottom DBR is composed of six pairs of alternating TiO_2 ($n = 2.2$) and SiO_2 ($n = 1.5$) layers, each of one-quarter wavelength optical thickness at a design wavelength of 962 nm. On top of the bottom DBR, a TiO_2 dielectric layer and a silver layer with a thickness of $d_t = 140$ nm and $d_{Ag} = 30$ nm, respectively, are deposited. Then, a cavity with length of d_c is formed with a top DBR having the same parameters as those of the bottom DBR. At last, a gold nanowire array with a periodicity of $p = 200$ nm along the x-axis is incorporated in the cavity, and placed 30 nm above the silver layer. In our analysis, the gold nanowires have a cross section of 100 nm × 20 nm. The whole structure is assumed to be infinite along the y direction, and illuminated by a TE- or TM-polarized (electric or magnetic field parallel to the y-axis) plane wave from top to bottom at normal incidence. All spectra and field distributions are calculated by employing rigorous coupled wave analysis (RCWA) [16,17], and the wavelength-dependent complex dielectric constants of gold and silver are taken from [18].

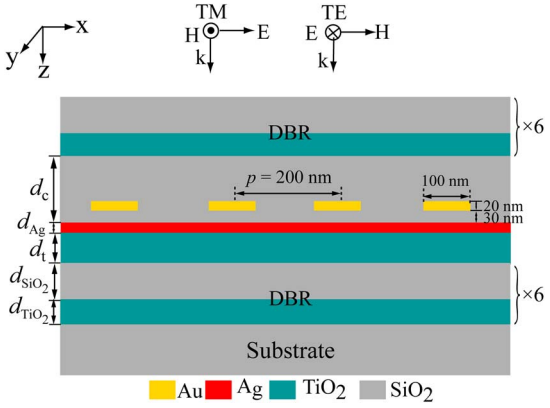

Fig. 1. Schematic view of the composite metal nanostructures studied in this paper.

3. PLASMON RESPONSE OF A MICROCAVITY WITH AN INTRACAVITY METAL LAYER

Figures 2(a) and 2(b) present the normal-incidence reflection and transmission spectra of a microcavity with or without an intracavity metal layer. The thickness of the cavity layer is taken as $d_c = 295$ nm. In the absence of a metal layer, a single cavity resonance, as well as two broad DBR sidebands, is observed. When a 30 nm metal layer is embedded into the microcavity, the original cavity resonance is transformed into two optical resonances. These coupled states are hybrid modes of the TPs and the cavity mode [8], labeled as TP I and TP II, respectively. Their eigenenergies depend on both the thicknesses of the metal layer and the adjacent dielectric layers. Figure 3 displays the normalized electric and magnetic field intensity distributions along the direction normal to the microcavity plane for these two hybrid TP modes. Upon the excitation of the TP I mode, it is observed that the electric fields are enhanced greatly at the center of the cavity [Fig. 3(a)], while the magnetic fields are highly enhanced at the interface between the cavity and the metal layer [Fig. 3(b)]. On the other hand, electric field intensities of the TP II mode [Fig. 3(c)] have a peak in the TiO_2 dielectric layer close to the metal layer, and the magnetic field intensity distribution [Fig. 3(d)] exhibits a maximum at the other interface of the metal layer. The electric or magnetic field intensity enhancement factor of TP II is much smaller than that of TP I.

Furthermore, when a gold nanowire array is embedded in the cavity and placed close to the metal layer, because of the

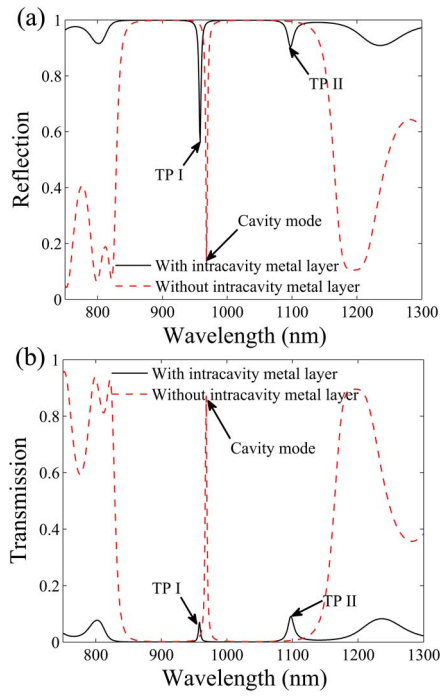

Fig. 2. (a) Reflection and (b) transmission spectra for a microcavity with (solid line) or without (dashed line) an intracavity metal layer at normal incidence.

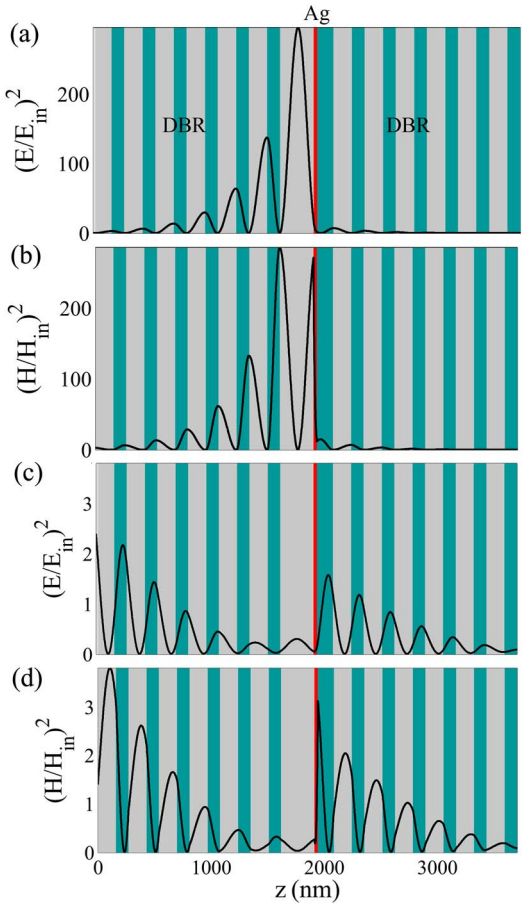

Fig. 3. (a) and (b) Normalized electric and magnetic field intensity distributions along the z direction of the microcavity with an intracavity metal layer for the TP I mode. (c) and (d) Normalized electric and magnetic field intensity distributions along the z direction of the microcavity with an intracavity metal layer for the TP II mode.

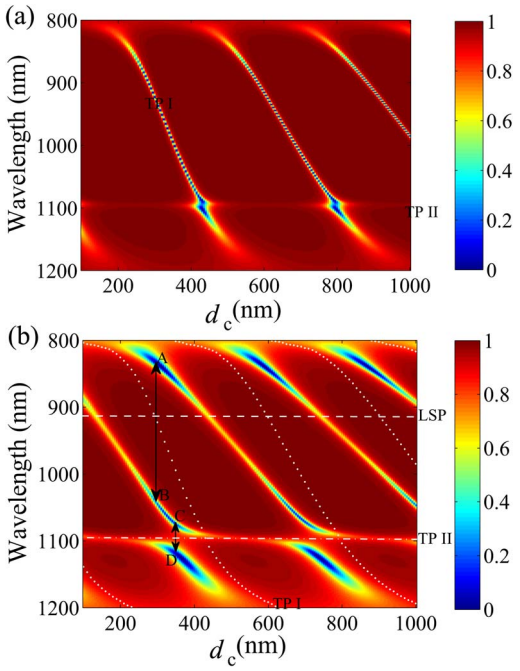

Fig. 4. Contour plots of the reflection versus wavelength and cavity layer thickness (d_c) for the considered structure consisting of a metallic nanowire array incorporated into a microcavity with an intracavity metal layer, illuminated by the (a) TE- and (b) TM-polarized light at normal incidence. In panel (b), the horizontal dashed and dashed-dotted lines denote the resonance positions of the unperturbed LSP and TP II modes, respectively; the dotted lines denote the resonance positions of the unperturbed TP I mode; the black arrows indicate splittings caused by mode couplings.

interaction of the LSPs excited on the nanowires with their dipole images in the metal layer [19,20], the electromagnetic fields can be highly confined and enhanced in the space between the nanowires and the metal film. Thus, strong coupling between the LSP and the TP I mode may be achieved in the considered structure because of large spatial overlap of their mode fields, and the electromagnetic field enhancements in the nanowire film space associated with excitation of the hybrid TP-LSP state can be very large.

4. CAVITY THICKNESS CONTROLLED LSP-HYBRID TPS MODE COUPLING

As previously reported [8], the eigen-energies of the TP I mode depend on the thickness of the cavity layer. To investigate the coupling between the LSP mode and these hybrid TP modes, in Fig. 4 we present the contour plots of the reflection versus wavelength and cavity layer thicknesses d_c for the considered structure shown in Fig. 1, illuminated by TE- or TM-polarized light at normal incidence. For TE polarization, the LSPs of the nanowires cannot be excited; only TP I and TP II modes can be formed. It is observed in Fig. 4(a) that multiple-order TP I modes exist in the considered range of cavity layer thicknesses. With the increase of d_c, the resonance wavelength of the TP I mode periodically increases, while that of the TP II mode remains unchanged, and an anticrossing behavior, as well as a small splitting, can be seen when the resonance wavelengths of TP I and TP II are approximately equal. These results indicate that the coupling between the TP I and TP II modes is relatively weak. The reason is that the TP I and TP II modes are separately formed on the opposite interfaces of the intracavity metal layer; the coupling between the TP I and TP II modes mainly depends on the frustrated decay of optical fields through the metal layer. Therefore, the coupling strength between these two hybrid TP modes is limited by the thickness of the intracavity metal layer.

Figure 4(b) shows the reflection spectra of the considered structure for TM polarization. In this situation, besides the two hybrid TP modes formed on the interfaces of the metal layer, an LSP located at $\lambda = 915$ nm can be excited on the gold nanowire array. In the figure, the resonant positions of the unperturbed LSP excited on a metallic nanowire array coupled to a metal film are depicted as a horizontal dashed line, and those of the unperturbed TP I and TP II are extracted from Fig. 4(a), and denoted by dotted lines and a horizontal dashed-dotted line, respectively. With the increase of d_c, anticrossing of the resonance positions is observed when the resonance wavelengths of the TP I and the LSP are approximately equal,

showing a splitting of 299 meV (indicated by the longer black arrow) at $d_c = 295$ nm, which is a signature of the strong coupling between the TP I mode and the LSP mode. In addition, the coupling results in two branches of new hybrid modes, called TP I-LSP hybrid modes in the following. With a further increasing in d_c, an anticross behavior is also observed at $d_c = 350$ nm between the lower branch TP I-LSP hybrid mode and the TP II mode, and the splitting [denoted by the shorter black arrow in Fig. 4(b)] caused by the coupling between these two modes is much larger than that between the TP I and TP II modes shown in Fig. 4(a). This means that the coupling between TP I and TP II can be enhanced greatly by embedding gold nanowires into the cavity with an intracavity metal layer. The underlying mechanism will be explained in the following.

5. MODE SPLITTING AND THE NATURE OF THE FORMED HYBRID MODES

In Figs. 5(a) and 5(b), the reflection and transmission spectra of the studied structure are plotted, respectively, at a cavity length of $d_c = 295$ nm for TE and TM polarizations, assuming normal light incidence. For the sake of comparison, those of the structure without incorporated nanowires are shown by the dashed curves. For TE polarization, only TP I and TP II modes can be formed. It is observed that the resonance wavelength of TP I mode is blue shifted when Au nanowires are incorporated, and the depth of the reflection dip caused by the excitation of TP I mode is increased drastically. At the same time, the corresponding transmission is very low, indicating a high narrow band absorption of TE polarization light at the TP I mode. For TM polarization, the resonance wavelength of TP I corresponds to that of the LSP at this cavity length, and the splitting of TP I into two new TP I-LSP hybrid modes, labeled as A and B, can be directly observed. These two hybrid modes result in two deep dips in the reflection spectrum, as well as two very low peaks in the transmission spectrum, which indicates that the proposed multilayer structure has an extra potential application in tunable multi-band absorbing polarization filters. Furthermore, the amplitude of the reflection dip or transmission peak associated with TP II is also increased largely in this situation. This means that, because of the coupling between the LSP and TP I, light can also be coupled to the TP II mode more easily.

Figures 6(a) and 6(b) show the normalized electric and magnetic field intensity distributions of the TP I mode, respectively, in the studied structure with incorporated nanowires for TE polarization. It is observed that the incorporated nanowires

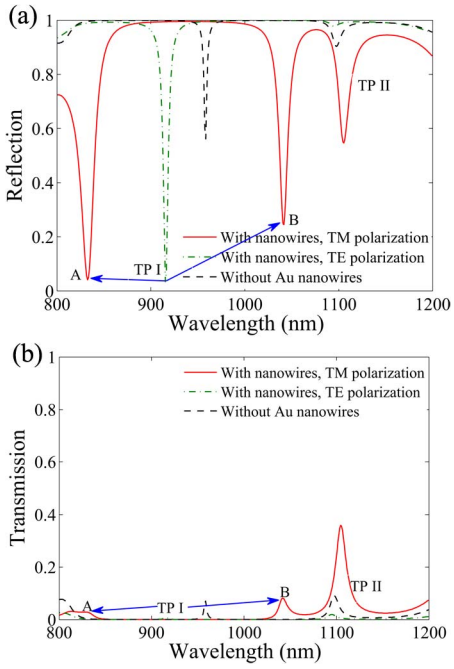

Fig. 5. (a) Reflection and (b) transmission spectra of the studied structure with incorporated nanowires for TE and TM polarizations, and normal light incidence, at $d_c = 295$ nm where strong coupling between TP I and LSP happens. As a comparison, the corresponding reflection and transmission spectra of the studied structure without incorporated nanowires are shown by dashed curves.

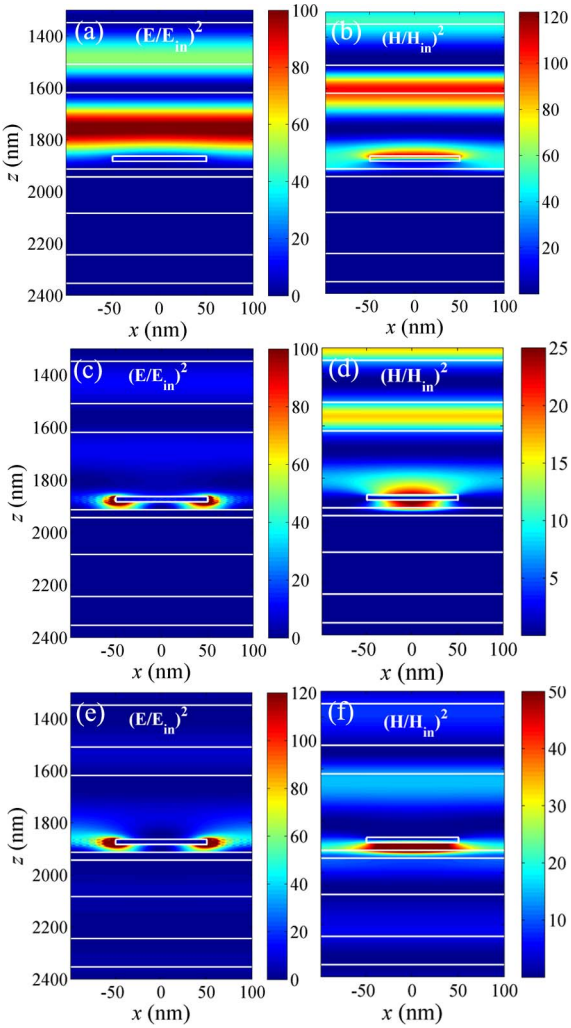

Fig. 6. (a) and (b) Normalized electric and magnetic field intensity distributions of the TP I mode in the studied structure with incorporated nanowires for TE polarization. (c) and (d) Normalized electric and magnetic field intensity distributions of the hybrid TPI-LSP mode labeled as A for TM polarization. (e) and (f) Same as (c) and (d), respectively, but for the hybrid TP I-LSP mode labeled as B. White lines denote the cross section of the structures.

have a negligible influence on the electric field intensity distribution; the electric fields are mainly confined in the cavity, the same as that of the structure without incorporated nanowires shown in Fig. 3(a), while the magnetic fields are highly enhanced near the top surface of the nanowires. However, for TM polarization, because of coupling with the LSP, the electric fields of the hybrid TPI-LSP mode labeled as A are highly confined and enhanced at the wire edges, and the magnetic fields are strongly localized into the space between the nanowires and the metal film as shown in Figs. 6(c) and 6(d), which is the signature of the LSP excited on the metal nanowires.

While the B mode features both the TP I and the LSP characteristics [see Fig. 6(e) and 6(f)]. First, because of the coupling with the TP I mode, the electric fields near the metal nanowire edges are further enhanced [see Fig. 6(e)], and the maximum electric field intensity is about 2.6 times that obtained by the excitation of the LSP on a metallic nanowire array coupled with a metal film (not shown here). Second, the electric field intensity also exhibits peaks in the center of the cavity, as well as at the interfaces between the TiO_2 and SiO_2 layers of the top DBR, a signature of the TP I mode. On the other hand, as shown in Fig. 6(f), the magnetic fields underneath the metal nanowires are significantly enhanced upon the excitation of mode B, and the maximum field intensity is about 4.3 times that obtained by the excitation of the LSP on a metallic nanowire array coupled with a metal film (not shown here). In this situation, the electromagnetic fields penetrating through the metal layer are enhanced greatly, and this is the reason why the coupling between TP I and TP II is enhanced greatly with the gold nanowire array incorporated. In addition, the magnetic fields are also enhanced on the top interface of the metal film and the interface between the cavity and the top DBR, also a signature of the TP I mode.

When the cavity length increases to $d_c = 350$ nm, the resonance wavelength of the lower branch TP I-LSP hybrid mode and that of the TP II mode are approximately equal; the reflection and transmission spectra of the studied structure are shown in Figs. 7(a) and 7(b), respectively, assuming normal light incidence and TM polarization. For a comparison, those of the structure without incorporated nanowires are shown by dashed lines. It is observed that the TP II mode is split into two well-separated hybrid modes C and D because of the coupling with the lower branch TP I-LSP hybrid mode. These two hybrid modes result in two deep dips in the reflection spectrum, and the structure has relatively high transmissions (> 0.5) at these two hybrid modes. In Fig. 8, we show the normalized electric and magnetic field intensity distributions of these two hybrid modes, labeled as C and D. Obviously, both the C and D modes feature the lower branch TP I-LSP hybrid mode and the TP II mode characteristics; namely, their magnetic field intensities are confined within the space underneath the nanowires and to both sides of the metal layer.

6. COUPLING MECHANISM EXPLANATION

To better understand the coupling mechanism, the dependence of the resonance positions of the coupled system on the cavity length d_c is calculated using a coupled oscillator model [21], which describes the coupling behavior of the original "bare"

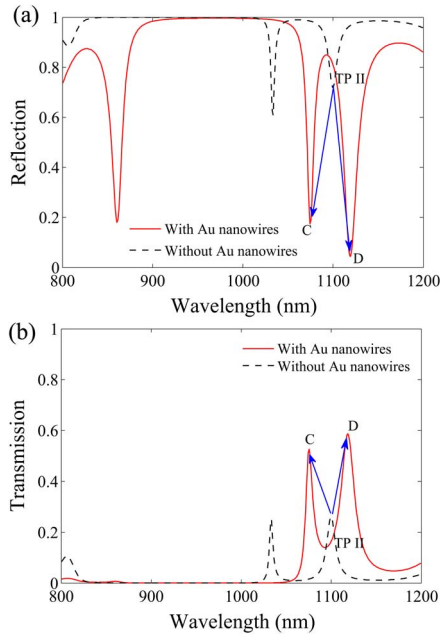

Fig. 7. (a) Reflection and (b) transmission spectra of the studied structure with incorporated nanowires for TM polarization and normal light incidence, at $d_c = 350$ nm, where strong coupling between the lower branch TP I-LSP hybrid mode and the TP II mode occurs. As a comparison, the corresponding reflection and transmission spectra of the studied structure without incorporated nanowires are shown by dashed curves.

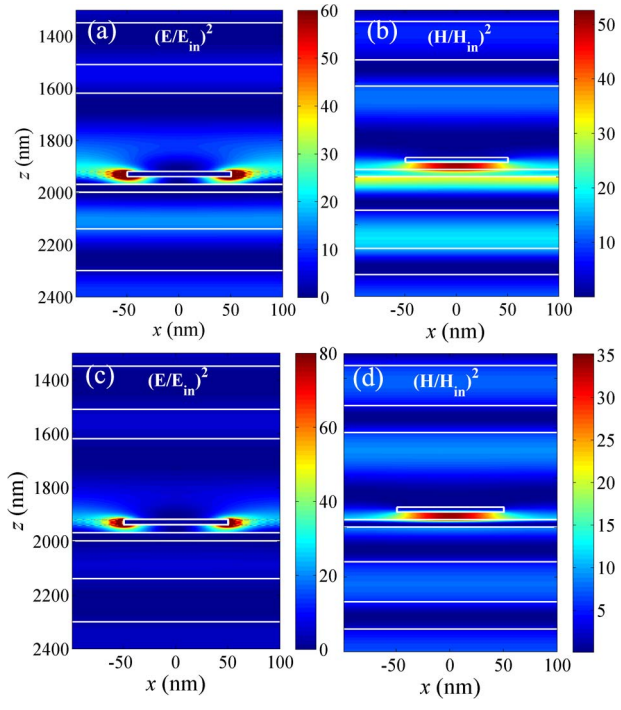

Fig. 8. (a) and (b) Normalized electric and magnetic field intensity distributions of the hybrid mode labeled as C in the studied structure for TM polarization. (c) and (d) Same as (a) and (b), respectively, but for the hybrid mode labeled as D. White lines denote the cross section of the structures.

modes in the system. The corresponding bare modes are the LSPs, the TP I modes, and the TP II modes. The effective Hamiltonian at normal incidence can be written as

$$H = \begin{pmatrix} E_{\mathrm{TPI}} & V_1 & V_2 \\ V_1 & E_{\mathrm{TPII}} & 0 \\ V_2 & 0 & E_{\mathrm{LSP}} \end{pmatrix}, \quad (1)$$

where E_{TPI}, E_{TPII}, and E_{LSP} are the energies of the uncoupled TP I, TP II, and LSP modes, respectively. V_1 is the coupling energy between the TP I and the TP II, and V_2 is the coupling energy between the TP I and the LSP mode. The coupling behavior can be described by introducing V_1 and V_2, and their amplitudes can be estimated from the energies of the splittings shown in Fig. 4(b).

The eigenvalues of the Hamiltonian represent the new eigenenergies of the coupled system. By taking the coupling strength to be $V_1 = 30$ meV and $V_2 = 150$ meV, the dependence of resonance positions on the d_c obtained by the coupled oscillator model is shown by the lines of red crosses in Fig. 9. For a comparison, the resonance positions extracted from the calculated reflection spectra [shown in Fig. 4(b)] are shown by the open circle lines. Clearly, we observe a good agreement between the positions obtained by the coupled oscillator model and those extracted from the reflection spectra. The red curved lines denote the positions of the uncoupled TP I mode, while the horizontal dashed and dashed-dotted lines denote the positions of the unperturbed LSP and TP II modes, respectively. At the crossings of the lines of the LSP and the TP I, the resonance positions present obvious anticrossings, which is a signature of the strong coupling between the LSP and the TP I mode. Furthermore, the coupling results in two branches of new TP I-LSP hybrid modes, and anticrossings between the lower branch TP I-LSP hybrid mode and the TP II mode are also observed; the formed splittings are much larger than those between the TP I mode and the TP II mode shown in Fig. 4(a). This indicates that the coupling between the TP I and TP II modes are enhanced greatly because of the incorporation of the nanowires in the desired structure.

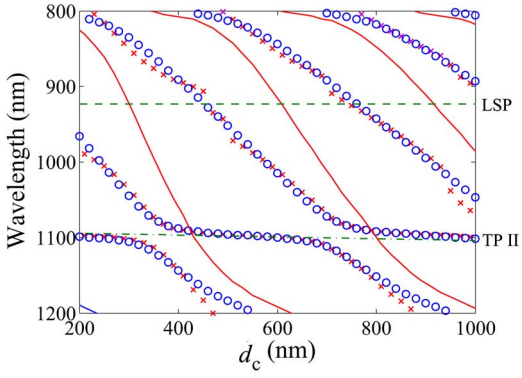

Fig. 9. Dependence of the resonance positions of the coupled system on the cavity length d_c. The lines of red crosses indicate the predicted resonance positions obtained by the coupled oscillator model. The open circles in blue indicate the reflection positions extracted from the calculated reflection spectra shown in Fig. 4(b). The horizontal dashed and dashed–dotted lines denote the positions of the unperturbed LSP and TP II modes, respectively. The red curved lines denote the positions of the uncoupled TP I mode.

7. CONCLUSION

In conclusion, we have demonstrated that strong coupling between LSPs and hybrid TPs can be achieved by incorporating a metallic nanowire array into a microcavity with an intracavity metal layer, and the couplings can be tuned by changing the cavity length. At appropriate cavity lengths, strong coupling between LSPs and TPs results in large anticrossings in the reflection spectrum, as well as two branches of TP-LSP hybrid modes. Upon the excitation of the TP-LSP hybrid mode, the electromagnetic fields are enhanced significantly in the space between the nanowires and the metal layer. Because of coupling with the LSP mode, the coupling between the two types of hybrid TPs is also enhanced greatly. Furthermore, the observed coupling behavior is well explained using a coupled oscillator model. These findings have potential applications in enhancing optical nonlinearity and reducing lasing threshold in organic microcavities.

Funding. National Natural Science Foundation of China (NSFC) (U1435210); Science and Technology Innovation Foundation of CAS (CXJJ-15Q071); Science and Technology Innovation Project of CIOMP (Y3CX1SS143).

REFERENCES

1. M. Kaliteevski, I. Iorsh, S. Brand, R. A. Abram, J. M. Chamberlain, A. V. Kavokin, and I. A. Shelykh, "Tamm plasmon-polaritons: possible electro-magnetic states at the interface of a metal and a dielectric Bragg mirror," Phys. Rev. B **76**, 165415 (2007).
2. M. E. Sasin, R. P. Seisyan, M. A. Kalitteevski, S. Brand, R. A. Abram, J. M. Chamberlain, A. Y. Egorov, A. P. Vasil'ev, V. S. Mikhrin, and A. V. Kavokin, "Tamm plasmon polaritons: slow and spatially compact light," Appl. Phys. Lett. **92**, 251112 (2008).
3. W. L. Zhang and S. F. Yu, "Bistable switching using an optical Tamm cavity with a Kerr medium," Opt. Commun. **283**, 2622–2626 (2010).
4. B. Auguié, M. C. Fuertes, P. C. Angelomé, N. L. Abdala, G. J. A. A. Soler Illia, and A. Fainstein, "Tamm plasmon resonance in mesoporous multilayers: toward a sensing application," ACS Photon. **1**, 775–780 (2014).
5. C. Symonds, A. Lemaıtre, P. Senellart, M. H. Jomaa, S. A. Guebrou, E. Homeyer, G. Brucoli, and J. Bellessa, "Lasing in a hybrid GaAs/silver Tamm structure," Appl. Phys. Lett. **100**, 121122 (2012).
6. C. Symonds, G. Lheureux, J. P. Hugonin, J. J. Greffet, J. Laverdant, G. Brucoli, A. Lemaitre, P. Senellart, and J. Bellessa, "Confined Tamm plasmon lasers," Nano Lett. **13**, 3179–3184 (2013).
7. T. Liew, A. Kavokin, T. Ostatnicky, M. Kaliteevski, I. Shelykh, and R. Abram, "Exciton-polariton integrated circuits," Phys. Rev. B **82**, 033302 (2010).
8. R. Brückner, M. Sudzius, S. I. Hintschich, H. Frob, V. G. Lyssenko, and K. Leo, "Hybrid optical Tamm states in a planar dielectric microcavity," Phys. Rev. B **83**, 033405 (2011).
9. M. A. Kaliteevski, A. A. Lazarenko, N. D. Il'inskaya, Y. M. Zadiranov, M. E. Sasin, D. Zaitsev, V. A. Mazlin, P. N. Brunkov, S. I. Pavlov, and A. Y. Egorov, "Experimental demonstration of reduced absorption of light by intracavity metallic layers," Plasmonics **10**, 281–284 (2015).
10. R. Brückner, A. A. Zakhidov, R. Scholz, M. Sudzius, S. I. Hintschich, H. Froeb, V. G. Lyssenko, and K. Leo, "Phase-locked coherent modes in a patterned metal-organic microcavity," Nat. Photonics **6**, 322–326 (2012).
11. A. Mischok, R. Brückner, M. Sudzius, C. Reinhardt, V. G. Lyssenko, H. Frob, and K. Leo, "Photonic confinement in laterally structured

metal-organic microcavities," Appl. Phys. Lett. **105**, 051108 (2014).
12. H. Liu, X. Sun, F. Yao, Y. Pei, H. Yuan, and H. Zhao, "Controllable coupling of localized and propagating surface plasmons to Tamm plasmons," Plasmonics **7**, 749–754 (2012).
13. B. I. Afinogenov, V. O. Bessonov, A. A. Nikulin, and A. A. Fedyanin, "Observation of hybrid state of Tamm and surface plasmon-polaritons in one-dimensional photonic crystals," Appl. Phys. Lett. **103**, 061112 (2013).
14. R. Das, T. Srivastava, and R. Jha, "Tamm-plasmon and surface-plasmon hybrid-mode based refractometry in photonic bandgap structures," Opt. Lett. **39**, 896–899 (2014).
15. M. Lopez-Garcia, Y. L. D. Ho, M. P. C. Taverne, L. F. Chen, M. M. Murshidy, A. P. Edwards, M. Y. Serry, A. M. Adawi, G. J. Rarity, and R. Oulton, "Efficient out-coupling and beaming of Tamm optical states via surface plasmon polariton excitation," Appl. Phys. Lett. **104**, 231116 (2014).
16. M. G. Moharam, E. B. Grann, D. A. Pommet, and T. K. Gaylord, "Formulation for stable and efficient implementation of the rigorous coupled wave analysis of binary gratings," J. Opt. Soc. Am. A **12**, 1068–1076 (1995).
17. M. G. Moharam, D. A. Pommet, and E. B. Grann, "Stable implementation of the rigorous coupled-wave analysis for surface-relief gratings: enhanced transmittance matrix approach," J. Opt. Soc. Am. A **12**, 1077–1086 (1995).
18. P. B. Johnson and R. W. Christy, "Optical constants of the noble metals," Phys. Rev. B **6**, 4370–4379 (1972).
19. G. Lévêque and O. J. F. Martin, "Optical interactions in a plasmonic particle coupled to a metallic film," Opt. Express **14**, 9971–9981 (2006).
20. A. Christ, T. Zentgraf, S. G. Tikhodeev, N. A. Gippius, J. Kuhl, and H. Giessen, "Controlling the interaction between localized and delocalized surface plasmon modes: experiment and numerical calculations," Phys. Rev. B **74**, 155435 (2006).
21. A. Christ, S. G. Tikhodeev, N. A. Gippius, J. Kuhl, and H. Giessen, "Waveguide-plasmon polaritons: strong coupling of photonic and electronic resonances in a metallic photonic crystal slab," Phys. Rev. Lett. **91**, 183901 (2003).